Real-time and post-facto correction for differential aberrations in direct planet imaging by adaptive optics

J.-F. Sauvage, T. Fusco, G. Rousset, and C. Petit

Département d'Optique Théorique et Appliquée, ONERA BP 72, 92322 Chtillon, France
email: jean-francois.sauvage@onera.fr

Abstract. We present experimental results of a new procedure of measurement and pre-compensation of the non-common path aberrations in Adaptive Optics. A significant Strehl ratio increase (from 70 to 95.5 % in R band) is demonstrated.

Keywords. Adaptive optics, Wave-front sensing, Phase diversity.

1. Introduction

The correction of non-common path aberrations (NCPA) is one of the critical issues to achieve ultimate adaptive optics (AO) performance. These aberrations have to be measured by a dedicated tool in the imaging camera. An efficient way to obtain such a correction is to use phase diversity (PD) [1, 2, 3, 4]. They are then pre-compensated by a modification of the Wavefront Sensor (WFS) references in the AO loop to obtain the wavefront error at the scientific detector. It is clear that such a process imposes linear WFS and thus is well adapted to Shack Hartmann (SH) WFS. This approach has been successfully applied on NAOS-CONICA [3, 5, 6] and has led to a significant improvement of the global system performance. Even if a real improvement can be seen on pre-compensated images, a significant amount of aberrations are still not corrected. Several effects may explain such a limitation. Firstly, phase diversity measurements are not perfect (due to noise effects, detector transfert function and algorithm approximations [3]). An optimized Phase Diversity algorithm is proposed in section 2. In addition, the pre-compensation of these measured aberrations is only partial due to uncertainties on AO models (WFS, Deformable Mirror (DM)). In order to avoid these model uncertainty effects (which are probably the more important limitation of the approach), a pseudo-closed loop scheme is proposed in section 3 for the measurement and the correction of NCPA. These new procedure is experimentally validated on the ONERA AO bench.

2. NCPA measurements

Phase Diversity [1] is a focal plane wavefront sensor able to estimate the pupil phase thanks to focal plane images of an artificial point source. In order to remove undetermination in the phase estimation, two focal plane images differing from a known aberration are needed. In our case, the known aberration is the defocus because of its simplicity to implement. A modification of the SH WFS reference slopes allows us to introduce or not the defocus on the DM by closing the loop on an artificial calibration source.

A PD algorithm [3] is used to measure NCPA on focused and defocused images i_f and i_d. We propose here a new optimized algorithm for the phase estimation. It is based on

a MAP approach, by maximizing the probability of obtaining simultaneously the object o and the phase ϕ knowing the images i_f and i_d. This probability can be rewritten as shown in equation 2.1 in order to introduce the *a priori* on the object and the phase $f(o)$ and $f(\phi)$:

$$f(i_f, i_d, o, \phi) = f(i_f, i_d | o, \phi) f(o) f(\phi) \tag{2.1}$$

The *a priori* knowledge on object is taken equal to 1 (meaning taht we assume the object to be totally unknown), but the *a priori* on the phase will take into account the phase spectrum in n^{-2} and constraint the noise error on high order Zernike modes. In practice, the algorithm minimizes the criterium $J(o, \phi)$ defined in equation 2.2 as the opposite of logarithm of the probability defined in 2.1 :

$$
\begin{aligned}
J(o, \phi) &= -\ln\left(f(i_f, i_d | o, \phi)\right) \tag{2.2}\\
&= -\ln\left(f(i_f, i_d | o, \phi)\right) - \ln\left(f(\phi)\right)\\
&= \left\| \frac{i_f(\vec{r}) - h_f(\phi, \vec{r}) * o(\vec{r})}{\sigma_f(\vec{r})} \right\|^2 + \left\| \frac{i_d(\vec{r}) - h_d(\phi, \phi_d, \vec{r}) * o(\vec{r})}{\sigma_d(\vec{r})} \right\|^2 + \phi^t R_\phi^{-1} \phi
\end{aligned}
$$

The expression of this criterium makes appear the noise standard deviation $\sigma_f(\vec{r})$ and $\sigma_d(\vec{r})$ in the focused and defocused images, with $\vec{r}$ the position vector in the image plane. This statistics allows us to deal with a non uniform gaussian noise, varying from one pixel to another , and modeling with a good approximation both photon and electronics noises. $h_f(\phi, \vec{r})$ and $h_d(\phi, \phi_d, \vec{r})$ are respectively the focused and defocused PSF of the intrument. h_f only depends on the aberrant phase ϕ and on the position vector, while h_d also depends on the known defocus phase ϕ_d.

The last term in equation 2.2 is the *a priori* knowledge on the phase : a typical spatial spectrum and phase variance, via the covariance matrix R_ϕ. The two different optimizations proposed here (non-uniform noise model and phase regularisation) are tested in section 3.

3. NCPA compensation

NCPA pre-compensation requires to compute the WFS slopes corresponding to the measured aberrations. These slopes are then substracted to te SH reference slopes, the new references being used in the closed loop operation. This slope modification requires a precise knowledge of the system parameters and a good model of the WFS itself. Any error on the WFS model directly affects the slope computation from measured NCPA and thus limits the performance of the global pre-compensation process. As an example, an error of 10% on the WFS pixel scale directly translates into an uncorrected error of 10% of the amplitude of the NCPA. These model errors are probably today the main limitation for the NAOS-CONICA system [5, 6].

3.1. *Pseudo-closed loop process*

3.1.1. Principle of the Pseudo- closed loop process

A first way to reduce these errors is of course to perform accurate calibrations of the WFS. Nevertheless, uncertainties on system parameters as well as remaining errors on calibrations will always degrade the ultimate performance of the pre-compensation process. In order to overcome this problem and to reach the ultimate performance in the NPCA pre-compensation process, a new approach is proposed. We called it the "pseudo closed loop" process.

The idea is to overcome model uncertainties using a multiple step process for the NCPA estimation and pre-compensation. First we perform a WFS calibration and we derive the initial WFS model. The pseudo closed loop approach can be summarized as follows:

1) first measurement of NCPA with PD
2) modification of reference slopes to account for NCPA using the WFS model
3) measurement of residual NCPA after the first pre-compensation
4) addition of the new slopes deduced from the residual NCPA to the current slopes
5) points 3) and 4) are performed until convergence. With such an approach, the only impact of the model uncertainties is to reduce the speed of convergence.

3.1.2. *First experimental validation*

The pseudo-closed loop process has been tested on the ONERA AO bench using the initial PD algorithm [3]. This laboratory bench is composed of a 9x9 actuator Deformable Mirror (DM) and a 8x8 sub-aperture SH-WFS. The imaging camera is a 512x512 Princeton camera with a 4e-/pixel/frame readout noise. A unresolved fibered laser diode source working at 630 nm, is used at the system entrance focal plane for calibration and closed-loop test.

The accuracy of the NCPA compensation is quantified thanks to Strehl ratio estimation in the focused images. The Strehl ratio is a widely used quality estimator for optical system, and is a way to quantify the residual phase in the pupil plane of the instrument. This Strehl ratio may be estimated in two different ways : firstly by a measurement SR_{im} in the focal plane image, and secondly by computing SR_{Zern} by using the PD measured coefficient (see equation 3.1).

$$SR_{Zern} = \exp(-\sum_{i=4}^{i=N} a_i^2) \tag{3.1}$$

with a_i the measured Zernike coefficients, and N the number of Zernike polynomials. Piston ($i = 1$) has no effect on image formation, Tip and Tilt ($i = 2, 3$) are interpreted as a movement of the observed object. The results presented in figure 1 show both the diminution of the measured Zernike coefficients with the number of iteration of the pseudo-closed loop process, and the increase of Strehl ratio with iteration number.

In our case, 75 Zernike coefficients are estimated (from a_4 to a_{78}) but only 33 are corrected (from a_4 to a_{36}) by the AO system because of the relatively small number of subapertures on the SHWFS. The large number of estimated coefficients also avoids aliasing effects coming from the high order Zernike modes estimated.

We plot on the figure 1 SR_{Im}, SR_{Zern} and the ratio between these two quantities, $SRim/SRzern$. The difference between SR_{Im} and SR_{zern} can be explained by the uncorrected high order coefficients (from a_{42} to a_{∞}) and the SR measurement bias due to mis-knowledge of the system (exact over-sampling factor, exact fibre size and shape). This ratio $SRim/SRzern$ is roughly constant whatever the iteration number is and its average value can be estimated to 98% which corresponds to a 15 nm rms phase error. We plot in figure 2 the PSF images obtained on the imaging camera without NCPA precompensation and after 1, 2 and 3 iterations of pseudo-closed loop NCPA corrections. It clearly shows the high order aberrations (we only compensate for 33 Zernike modes here). It is interesting to notice that the PSF structures far from the optical axis (due to the high order non-compensated aberrations) roughly remain the same whatever the number of iterations is, as expected (they remain uncorrected). The correction of low order aberrations allows us to clean the centre of the PSF. It tends to a perfect Airy pattern with two complete Airy rings and a third clearly visible.
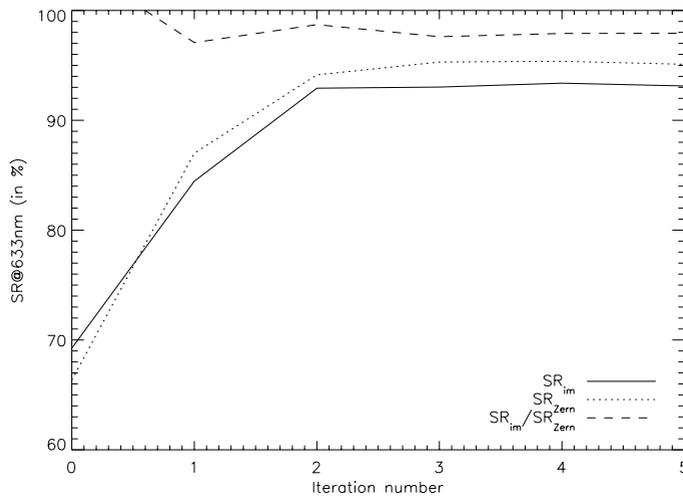
Figure 1. Experimental results of non-common path aberrations pre-compensation using phase diversity measurements and reference slope modifications. SR_{im} is measured on the focal plane PSF recorded at 633 nm. In addition, SR_{zern} computed from the measured NCPA is plotted in dotted line. The ratio between SR_{im} and SR_{zern} is plotted in dashed line.

Figure 2. PSF corresponding to the 4 first points of Fig 1, represented in invert logarithmic scale. The PSF on the left is the PSF obtained without any pre-compensation and used to perform the first PD measurement (iteration 0). The 3 other PSF correspond to iteration 1, 2 and 3 respectively. $\lambda = 632nm$.

3.2. *Tests of optimized algorithms*

Until now, the algorithm used to perform phase diversity was the classical one : uniform noise model, and no regularisation term [3]. We are going now to test the optimized algorithm with the non-uniform noise model and the phase regularisation with the experimental pseudo-loop procedure.

In order to test these algorithms, two different regimes of Signal to Noise Ratio (SNR) have been used. The SNR is defined as the ratio of the maximum of the focused image on the noise standard deviation.

• high SNR regime as in section 3, $SNR = 3 \times 10^4$ in order to test influence of photon noise on the non-uniform algorithm. This SNR regime ensures us that the predominant noise is the photon noise.

• low SNR regime, $SNR = 10^2$ (obtained with smallest exposure time while acquiring the pair of images) in order to test the gain brought by non-uniform noise and by regularisation.

Table 1 gathers the different level of Strehl Ratio after 5 iterations obtained with the different algorithm.

	Classical algorithm	Non uniform algorithm	Regularised algorithm	Regularised and non uniform algorithm
Saturation level for high SNR	93.5%	95.5%	93.5%	95.5%
Saturation level for low SNR	72.1%	81.2%	91.9%	92.3%

Table 1. SR values obtained with the different algorithms : classical, non-uniform, and regularised for high and low SNR regimes. Accuracy of SR measurement is estimated to 0.2% rms.

3.2.1. *Gain brought by non-uniform noise model*

The gain brought by non uniform noise model is revealed even for high SNR conditions. As in photon noise regime the noise variance evolves from one pixel to another, a non uniform algorithm is usefull to be more accurate in the Zernike coefficient measurements.

As written in table 1, the level reached with non uniform noise model at high SNR regime (95.5%) is higher than with the classical uniform algorithm (93.5%) at the same SNR regime. The use of non uniform model at low SNR regime brings a substantial gain of 9%.

At very high SNR the Phase diversity measurement is anyway very good even with the classical algorithm. The gain is therefore only 2% in Strehl Ratio, but such a gain at high SR is mandatory for the condition required by exoplanet detection.

3.2.2. *Gain brought by regularized algorithm*

The gain brought by the use of the regularisation term is revealed for low SNR regime. At low SNR, the classical algorithm without regularisation is unable to estimate correctly the phase and therefore the compensation is not efficient. The SR value remains at 72.1%. But with the use of regularisation, the SR value is at 91.9%, the NCPA have been estimated with almost the same accuracy than at high SNR regime with the classical algorithm.

4. Conclusion

The proposed new procedure for the measurements and the pre-compensation of the NCPA allows us to achieve a high performance (SR of 95.5%) on our own AO bench. This at the level of the requirement for extrem AO in order to detect exoplanets from the ground.

References

[1] R. A. Gonsalves, "Phase retrieval and diversity in adaptive optics," *Optical Engineering* **21**(5), pp. 829–832, 1982
[2] R. G. Paxman, T. J. Schulz, & J. R. Fienup, "Joint estimation of object and aberrations by using phase diversity," *Journal of the Optical Society of America A* **9**(7), pp. 1072–1085, 1992
[3] A. Blanc, T. Fusco, M. Hartung, L. M. Mugnier, & G. Rousset, "Calibration of NAOS and CONICA static aberrations. Application of the phase diversity technique," *Astron. Astrophys.* **399**, pp. 373–383, 2003

[4] A. Blanc, L. M. Mugnier, & J. Idier, "Marginal estimation of aberrations and image restoration by use of phase diversity," *J. Opt. Soc. Am. A* **20**(6), pp. 1035–1045, 2003

[5] G. Rousset, F. Lacombe, P. Puget, N. Hubin, E. Gendron, J.-M. Conan, P. Kern, P.-Y. Madec, D. Rabaud, D. Mouillet, A.-M. Lagrange, & F. Rigaut, "Design of the Nasmyth Adaptive Optics System (NAOS) of the VLT," in *Astronomical Telescopes & Instrumentation*, D. Bonaccini and R. K. Tyson, eds., **3353**, Proc. Soc. Photo-Opt. Instrum. Eng., (Kona, Hawaii), Mar. 1998

[6] M. Hartung, A. Blanc, T. Fusco, F. Lacombe, L. M. Mugnier, G. Rousset, & R. Lenzen, "Calibration of NAOS and CONICA static aberrations. Experimental results," *Astron. Astrophys.* **399**, pp. 385–394, 2003